Research Square

Preprints are preliminary reports that have not undergone peer review.
They should not be considered conclusive, used to inform clinical practice,
or referenced by the media as validated information.

W-Plated Kevlar Composites Inspired by Lamellar Armor: Experimental Ballistic Evaluation Under Modified NIJ IIA Conditions

Lucas Choi

27.lucas.choi@yisseoul.org

Yongsan International School of Seoul

Anshuman Das

Massachusetts Institute of Technology

Research Article

Keywords: Protective product design, Kevlar composites, Lightweight armor, W-Plating, Lamellar armor

Posted Date: June 26th, 2026

DOI: https://doi.org/10.21203/rs.3.rs-10028087/v1

License: This work is licensed under a Creative Commons Attribution 4.0 International License.
Read Full License

Additional Declarations: No competing interests reported.

Version of Record: A version of this preprint was published at Discover Materials on October 28th, 2026.
See the published version at https://doi.org/10.1007/s43939-026-01043-1.

W-Plated Kevlar Composites Inspired by Lamellar Armor: Experimental Ballistic Evaluation Under Modified NIJ IIA Conditions

Lucas Choi[ORCID: 0009-0006-5738-5513][1] and Anshuman Das[Google Scholar][2]
[1)] *Yongsan International School of Seoul*®[a)]
[2)] *Former Researcher, Camera Culture Group, MIT Media Lab, Massachusetts Institute of Technology*[b)]

(*Electronic mail: 27.lucas.choi@yisseoul.org)

(Dated: 18 June 2026)

ABSTRACT

Kevlar is one of the most widely used materials in modern body armor due to its high strength-to-weight ratio [1, 2]. This study explores a lightweight composite armor architecture inspired by medieval armor principles using vertically stacked W-shaped plates to investigate the influence of segmented geometry on composite armor behavior. Quasi-static compression testing was conducted using a 6000-series alignment fixture to measure load-displacement and energy absorption. Ballistic testing at Element U.S. Space & Defense Laboratories followed a modified National Institute of Justice (NIJ) 0101.06 Level IIA protocol, and coupons resisted penetration by six 9 mm, 124-grain full metal jacket (FMJ) projectiles at velocities ($\sim$ 1,200 ft/s). Five impacts produced negligible measured backface deformation (<1 mm) below the 44 mm maximum specified under NIJ 0101.06 [3], while one impact resulted in 57 mm deformation without projectile penetration. Microstructural analysis indicated preserved fiber integrity and interlayer bonding following testing. Collectively, the experimental findings indicate coupon-scale ballistic resistance under modified NIJ Level IIA conditions and support further investigation of geometry-driven composite armor architectures through larger-scale testing.

Keywords: Protective product design, Kevlar composites, Lightweight armor, W-Plating, Lamellar armor

I. INTRODUCTION

From medieval lamellar constructions to modern Kevlar composites, armor designs have had to balance protection, flexibility, and mobility. Medieval lamellar armors achieved this balance through hundreds of segmented plates with partial gaps [4–6], although steel substantially limited agility. The development of para-aramid fibers such as Kevlar in the 1960s enabled a transition from rigid metallic armor to high-strength fiber-based systems with substantially improved tensile strength-to-weight ratios, offering improved mobility relative to steel while maintaining ballistic and thermal resistance [7]. For higher-caliber threats, torso-centric rigid plates remain the standard [8]. However, this approach leaves peripheral regions vulnerable, and increasing coverage with rigid materials significantly reduces wearer mobility [9].

Hence, one limitation of contemporary armor systems lies in the reliance on monolithic and rigid plate geometries that reduce wearer mobility. Typically, armor can be categorized into two types: flexible, lightweight systems with limited structural reinforcement and rigid plate-based configurations offering higher ballistic resistance at the expense of mobility. Despite Kevlar's widespread adoption and its documented role in saving over 3,100 lives [10], coverage gaps persist in anatomically vulnerable regions such as the underarms and lateral torso, or the so-called "Achilles heel" of body armor [11].

In the quest for alternate designs, one could explore fictional armor systems in popular media that emphasize a creative balance between protection and flexibility. While such designs are typically speculative, they raise a legitimate engineering question: to what extent can modern composite materials and structural geometries remain lightweight while still providing meaningful ballistic protection. Prior engineering analyses suggest that concept-driven designs may be feasible when interpreted through modern materials science frameworks. For instance, Shin examined the theoretical possibility of translating a cinematic "Batsuit"-inspired concept into a real-world protective system using contemporary composite materials and design principles [12]. By re-imagining the strengths of 15th-century lamellar armor and replacing steel with lightweight Kevlar, these principles can be adapted to balance mobility and multi-directional protection that comes from Kevlar's innate properties.

To investigate the proposed hypothesis, a W-Plating armor architecture was developed to reinterpret segmented lamellar principles using lightweight Kevlar composites. Unlike material-focused approaches that prioritize fiber stacking and laminate thickness [8], the proposed design delves into plate geometry as a potential structural parameter influencing lightweight composite behavior.

The primary contribution of this work is the development and preliminary experimental evaluation of a geometry-driven W-Plated Kevlar composite architecture inspired by lamellar armor principles. The objective is to explore the influence of segmented plate geometry on impact response and deformation behavior through quasi-static compression, microstructural analysis, and modified NIJ Level IIA ballistic testing. The findings provide an initial foundation for future large-scale investigations of geometry-driven composite armor sys-

[a)] Principal Investigator, KALA Initiative (Kevlar Armor and Lightweight Applications)
[b)] Project affiliation with the MIT Media Lab Camera Culture Group: https://www.media.mit.edu/groups/camera-culture/overview/.



FIG. 1. Representative plate geometries used in early lamellar-inspired prototypes.

tems.

The proposed armor system was developed through iterative fabrication and testing cycles. Layered composite assemblies incorporating Kevlar fabrics, carbon-based sheets, and elastomeric substrates are prepared and evaluated [13, 14] to assess ballistic performance, deformation behavior, and structural integrity. Fabrication methods informed by specialized design and materials enable improved material integration and optimized plate geometries. Two primary prototype iterations are studied with alternative Kevlar stacking sequences, 3D-printed ABS polymer components, and impact-resistant EVA foam layers to quantify trade-offs among stiffness, energy absorption, flexibility, and overall mass.



FIG. 2. Fabrication and geometric organization of the W-Plating architecture.

A. Historical Modularity and Motion

Biomechanical analysis of late medieval armor shows that segmented overlapping plate systems preserved around 75% of normal gait efficiency, indicating that this configuration could maintain agile movement without compromising defense [15]. However, reliance on high-density steel ($\rho \approx 7.8\,\mathrm{g/cm^3}$) as the primary structural material imposed substantial mass penalties relative to modern aramid fiber composites ($\rho \approx 1.44\,\mathrm{g/cm^3}$) [1]. Thereby, the replacement of steel with lightweight Kevlar and the application of simplified geometries reduce mass while preserving material coverage relative to rigid steel systems. Early lamellar-inspired implementations have revealed that excessive inter-plate gaps resulted in vulnerabilities, thus motivating the development of a more coherent W-Plating structure to reduce gap-related failure while maximizing ballistic performance.

B. W-Plating Geometry

The W-Plating method is a vertically stacked, overlapping composite plate architecture composed of alternating convex–concave triangular segments inspired by biological and historical armor systems and developed to investigate the influence of segmented plate geometry on composite armor behavior [16–18]. Adjacent inter-plate gaps are minimal (2–3 mm) and are continuously bridged by underlying aramid fiber layers, maintaining continuous material coverage. No preferential failure was observed at inter-plate gaps under the tested conditions, and are intentionally maintained to impart torsional flexibility and reduce shear stress under bending.

II. METHODS

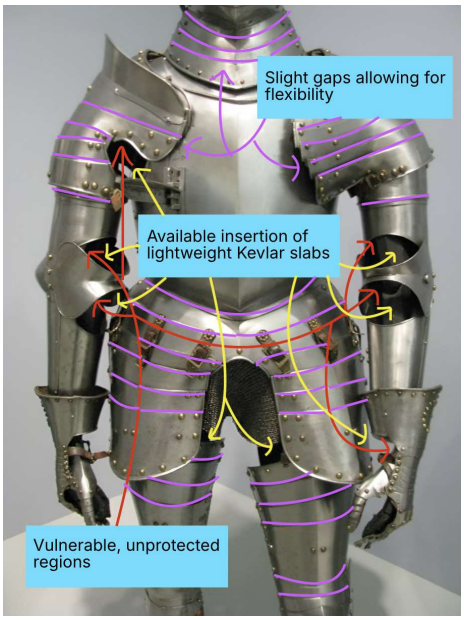


FIG. 3. Annotated representation of medieval segmented armor showing overlapping plate arrangements and load distribution principles relevant to flexible composite armor systems. Adapted from Ref. 19.

A. Reinforcement Strategies

Kevlar layups were oriented at $\pm 45^\circ$ to maximize multi-directional impact resistance against a broader range of threats, as summarized in Table 1. Critical torso regions employed epoxy-reinforced thick tri-weave Kevlar for structural

strength, while surrounding areas consisted of hand-stitched standard aramid fiber to maintain overall mobility. Shear thickening fluid (STF)-based systems have also demonstrated improved ballistic resistance in flexible armor configurations [20, 21]. Likewise, thin D3O and lightweight foam backings were incorporated to reduce BFD [22].

TABLE I. Design objectives, engineering challenges, and corresponding strategies incorporated into the W-Plated composite architecture.

Objective	Underlying Engineering Challenge	Implemented Strategy
Trauma mitigation	Concentrated force transfer during ballistic impact	Segmented W-shaped geometry to distribute loading across adjacent plates
Coverage continuity	Vulnerabilities in plate junctions	Continuous Kevlar substrate beneath articulated plate segments
Structural efficiency	Protection-to-mass trade-offs in wearable armor	Hybrid aramid composite construction with localized reinforcement
Energy dissipation	Direction-dependent deformation behavior	$\pm 45^{\circ}$ fiber orientation and multi-layer composite stacking

B. Prototype I: Preliminary Lamellar Composite Design

1. *Lamellar Composite Design and Construction*

Prototype I served as the baseline lamellar-style configuration and did not employ the W-Plating method. The lamellar assembly was constructed using traced and scaled pattern templates that comprised approximately 20 soft composite plates distributed across the torso and limbs, with a central chestplate with the thickest layering. Each plate comprised of 15 aramid Kevlar layers (0.66 mm, 3000 deniers) with $\sim$9 layers of triweave Kevlar and carbon fabrics/sheets along with 3-5 mm EVA foam. The plates were sewn to a mesh undersuit to allow breathability, and Kevlar-reinforced gloves were included for hand protection during emergency breakout scenarios.

2. *Quasi-Static Compression Testing*

Quasi-static compression testing was conducted to evaluate the stiffness and deformation behavior of Prototype I Kevlar composite plates under simulated blunt-force loading. The gray composite sample reached a peak load of 769 N at a displacement of 6.87 mm, indicating higher stiffness but reduced deformability, whereas the black composite sample reached a slightly lower peak load of 740 N with a displacement of 8.00 mm, demonstrating greater flexibility and enhanced energy absorption prior to failure, as shown in Fig. 5.



FIG. 4. Quasi-static compression testing of representative Kevlar composite plates using a 609 Alignment Fixture at Columbia University's Carleton Laboratory. The gray composite plate (Sample 2, left panel) consisted of approximately 7–9 Kevlar layers with increased epoxy and foam content to promote energy absorption, while the black composite plate (Sample 3, right panel) included 23 Kevlar layers with additional foam reinforcement to enhance structural rigidity.

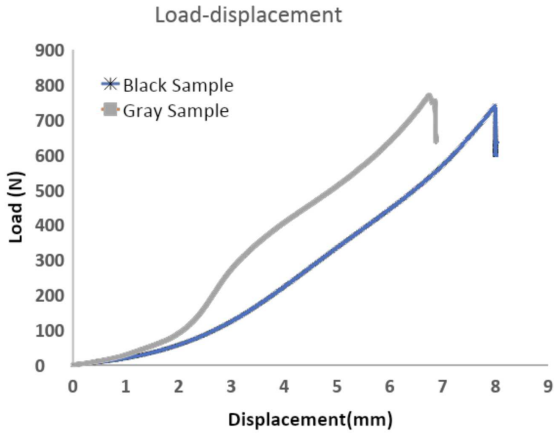


FIG. 5. Load–displacement response of Gray and Black composite plates under quasi-static compression. The gray plate exhibited a slightly higher peak load with reduced displacement, while the Black plate showed increased deformation and energy absorption prior to failure, corroborating the trade-off between stiffness and deformation-driven energy dissipation.

3. *Strength-Weight Ratio Analysis*

The strength-to-weight ratio analysis was included as a comparative quasi-static mechanical metric to evaluate relative structural efficiency among prototype configurations. Because quasi-static compression and ballistic impact involve fundamentally different loading regimes, these measurements should not be interpreted as direct predictors of ballistic performance or NIJ ballistic resistance.

$$\text{Strength-to-Weight Ratio} = \frac{F}{m}$$

F = Peak compressive load (N)
m = Mass of the object (kg)

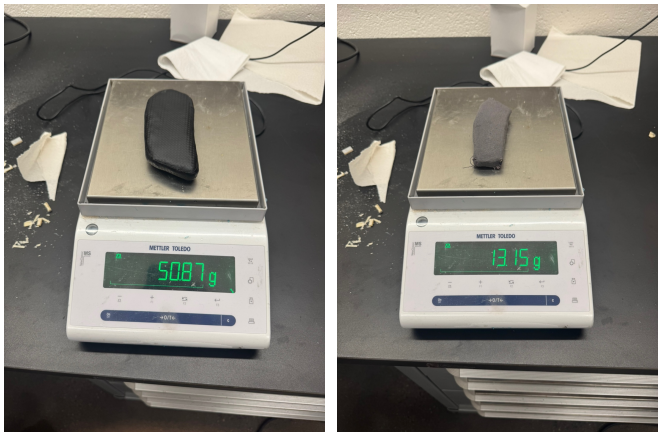


FIG. 6. Measured mass of black composite plate (Sample 3, left panel) and gray composite plate (Sample 2, right panel) at Columbia University's Carleton Lab.

$$\text{Strength-to-Weight Ratio}_{\text{Black}} = \frac{740.09\ \text{N}}{0.05087\ \text{kg}} \approx \boxed{14{,}552.4\ \text{N/kg}}$$

The black composite plate (Sample 3) exhibited a peak compressive load of 740.09 N, yielding a strength-to-weight ratio of approximately 14,552.4 N/kg. Although less mass-efficient than the gray plate, its greater mass (50.87 g) and larger surface area (83.91 cm²) were associated with a higher absolute load-bearing capacity during quasi-static compression.

$$\text{Strength-to-Weight Ratio}_{\text{Gray}} = \frac{769.12\ \text{N}}{0.01315\ \text{kg}} \approx \boxed{58{,}495.1\ \text{N/kg}}$$

The gray composite plate (Sample 2) achieved a strength-to-weight ratio of 58,495 N/kg while sustaining a peak compressive load of 769.12 N at a mass of 13.15 g. Relative to the black composite plate, the gray plate exhibited a higher load-to-mass ratio under quasi-static compression.

These results illustrate differences in mechanical compressive behavior between the tested configurations and should not be interpreted as evidence of superior ballistic performance.

C. W-Plating Concept

Central to this design is the development of the W-plating method, in which "W" shaped geometrical plates are vertically stacked, and aligned from top-to-bottom configuration. This horizontal, wide plate geometry was developed as a proof-of-concept segmented composite architecture for experimental evaluation under mechanical and ballistic loading conditions [23–25]. Additionally, the vertical alignment creates minimal seams between each plate, and these narrow gaps are strategically reinforced with lightweight ABS plastic, epoxy, and Kevlar slabs for articulation.

Because the W-Plating architecture was developed for broad, relatively flat regions such as the chest, abdomen, ribs, and back, high-mobility regions such as the shoulders, biceps, thighs, and neck employed alternative plate geometries. In these zones, curved, rectangular plates were integrated.

Although anatomical curvature and joint-rotation created larger gaps, flexible Kevlar fiber inserts were utilized to maintain coverage during dynamic movement, thus minimizing stiffness. These inserts replace hard materials, which can compromise flexibility and wearer comfort in regions such as the underarms, biceps, shoulders, and inner thighs.



FIG. 7. Close-up of W-Shaped Kevlar Plate Segment. Small inter-plate spacing (2–3 mm) is a design feature that permits articulation; continuous ballistic coverage is preserved via aramid fiber layers beneath the segmented plates.

Figure 7 shows a completed, hand-cut W-shaped Kevlar composite plate designed for torso application. The plate is composed of 20 stitched layers of aramid fiber, contoured for anatomical fit and directional flexibility. During the sealing process, epoxy bubbling was observed, revealing a fabrication challenge related to uneven adhesive distribution and trapped air. The fraying edges indicate the unfinished state of the material prior to trimming and before the addition of outer finishing layers such as premium leather and carbon sealant wraps.

D. Advanced Prototype II: W-Plating Engineering Implementation

Unlike Prototype I, which was mobility focused, Prototype II achieves a closer balance between mobility and protection. Prior studies report that Kevlar's tensile strength increases by 302.9 MPa (+30%) [26] when bonded with epoxy or resin. The advanced prototype was fabricated using the following steps:

(a) **Template Preparation:** Paper templates were sketched

to define plate geometry and anatomical coverage for critical regions including the ribs, neck, chest, and legs.

(b) **Kevlar Cutting and Fiber Orientation:** Kevlar fabric (3000 denier, 0.66 mm per layer) was cut according to the templates and layered at $\pm 45^{\circ}$ orientations to enhance multi-axial energy dissipation and directional impact resistance.

(c) **Layer Stacking Geometry Formation:** Between 15–27 Kevlar layers were stacked for each plate depending on the target protection zone. The stacked layers were then spliced into W-shaped segments.

(d) **Foam Integration:** Impact-resistant EVA foam (3–5 mm) was traced from the same templates and placed beneath the Kevlar composite to improve blunt-force absorption.

(e) **Epoxy Bonding:** Layers were bonded using a controlled epoxy application to improve fiber–matrix load transfer while maintaining flexural integrity.

(f) **Sealing and Encapsulation:** Each plate was sealed using premium leather and nylon-based textile wraps to protect against UV exposure, moisture, abrasion, and environmental degradation.

To optimize both flexibility and protection, plates in regions such as the chest, abdomen, and lower spine (Samples 1, 2, 5) were reinforced using a higher concentration of epoxy with thin, densely compacted laminates to enhance stiffness without significant mass increase. These vital zones function as structural shields against high-force contact. In contrast, less vital or high-mobility regions, such as the shoulders, arms, and sides, were constructed with thicker composite materials and soft-stitched flexible patterns to preserve articulation and comfort. This variation in stiffness created a dynamic system where protection adapted to anatomical function. The armor was thinner and more rigid in vulnerable regions, whereas it was thicker and more flexible in less critical areas.

E. Microstructural Characterization

1. *Scanning Electron Microscopy (SEM)*

Scanning electron microscopy (SEM) was conducted at the Stanford Nano Shared Facilities (SNSF) under the guidance of Dr. Tobi Beetz and Dr. Paul Hart to evaluate fiber-scale morphology and matrix–fiber interactions following impact and mechanical loading. The SEM images provide higher-resolution insight into aramid fiber continuity, surface condition, and localized deformation features.

2. *Optical Microscopy*

Optical microscopy was used to assess surface deformation and fiber-level damage in black and gray Kevlar composites following loading.



(a) Prototype I (lamellar-inspired)

(b) Prototype II (W-plating applied to torso)

FIG. 8. Comparison of armor prototypes showing (a) lamellar-inspired Prototype I and (b) Prototype II incorporating the W-Plating architecture in the torso region.



FIG. 9. Guard Biceps: Two prototype views showing alternative Kevlar reinforcement layouts for anatomically conformal upper-arm protection.



FIG. 10. Acrylonitrile Butadiene Styrene (ABS) shell chestplate

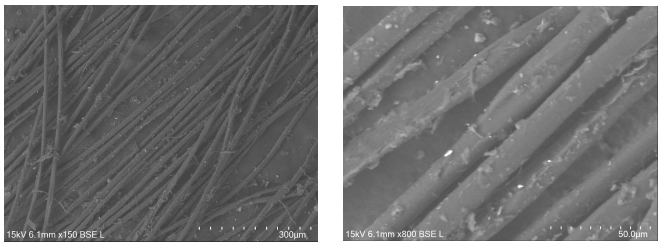
The 3D-printed ABS chestplate serves as a lightweight, impact-resistant outer shell layered above the internal Kevlar composites.



FIG. 11. Soft-composite chestplate

31 total layers: tri-weave and aramid Kevlar (0.66 mm, 3000 denier), carbon fiber sheets, leather, and EVA foam.

The black composite displays matrix-dominated cracking with localized densification, whereas the gray composite shows fiber pull-out and bundle separation. Laminate continuity is preserved in both configurations.



(a) (b)

FIG. 12. SEM micrographs of Kevlar fibers after loading. (a) Lower magnification showing largely continuous aligned fibers with adhered matrix residue. (b) Higher magnification showing localized surface roughening and debris consistent with matrix fragmentation and inter-fiber abrasion.

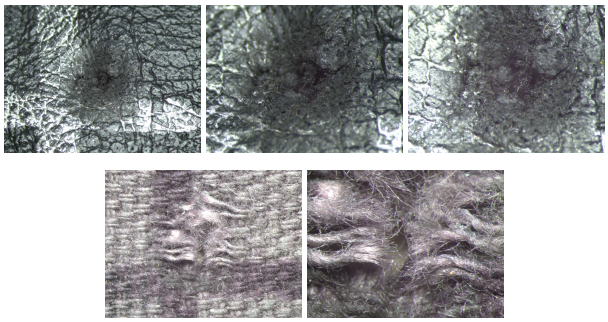


FIG. 13. Optical micrographs of black (top row) and gray (bottom row) composites. The black sample shows localized indentation and matrix cracking, while the gray sample exhibits fiber fraying and yarn-level disruption.

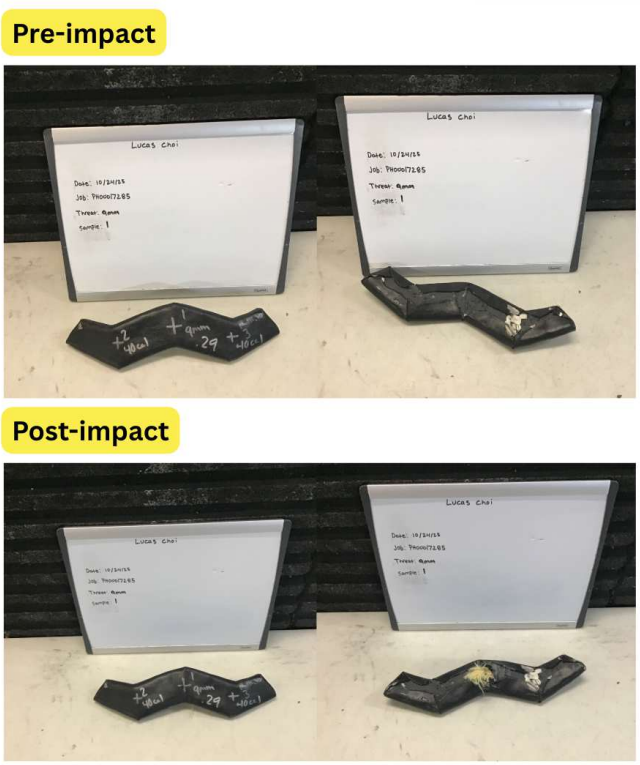


FIG. 14. Pre-impact condition of Sample 1 (W-Plated composite) following modified NIJ Level IIA ballistic testing.

F. Ballistic Testing (Element U.S. Space & Defense)

Ballistic testing was conducted at *Element U.S. Space & Defense Laboratories* (Belcamp, Maryland) to evaluate the impact resistance of the Kevlar-based composite armor prototypes. The ballistic evaluations were conducted under modified NIJ Level IIA-inspired conditions on reduced-scale coupon specimens, following a modified NIJ 0101.06 procedure using 9 mm FMJ rounds (124 grain) at velocities of approximately 1,195–1,255 ft/s (364–383 m/s). Test conditions included controlled velocity screening, clay witness backing, and ambient environmental conditions. Each sample was mounted against a calibrated Roma Plastilina No. 1 clay backing to measure BFD and simulate soft-tissue response under dynamic loading.

Due to the limited dimensions of the prototype coupons, the standard NIJ multi-hit spacing was proportionally scaled. Each sample received between one and two direct impacts. Ambient testing conditions were maintained at 69–70°F and 48% relative humidity.

Table II summarizes the coupon-level ballistic test outcomes. All five samples resisted projectile penetration by 9 mm FMJ rounds under the tested conditions. Four coupons exhibited no measurable BFD (<1 mm), and one coupon (Sample 3) showed 57 mm BFD without penetration. Sample 3 served as a material-thickness control (flat laminate, geometry not optimized), and the elevated BFD indicates that thickness alone does not ensure trauma mitigation. Collectively, these results demonstrate coupon-scale resistance to projectile penetration under the evaluated conditions, supporting further investigation of geometry-driven composite armor architectures.

TABLE II. Prototype I & II Ballistic Testing at Element U.S. Space & Defense (Belcamp, MD; 2025–10–24) Summary

Sample	Size (in)	Mass (g)	Shots	Vel. (ft/s)	Pen.	BFD (mm)
1 (W)	13.0×2.5	131.5	1	1198	None (spall)	≈0
2 (W)	4.0×1.5	9.07	1	1196	None (spall)	≈0
3 (Lamellar)	4.5×2.0	49.9	1	1199	None	57
4 (Hybrid)	7.5×4.5	86.2	1	1199	None (spall)	≈0
5 (Hybrid)	13.5×6.0	644.1	2	1203/1199	None (spall)	≈0

III. DISCUSSION

All five coupons resisted penetration of 9 mm 124 gr FMJ projectiles within the NIJ 0101.06 Level IIA velocity band

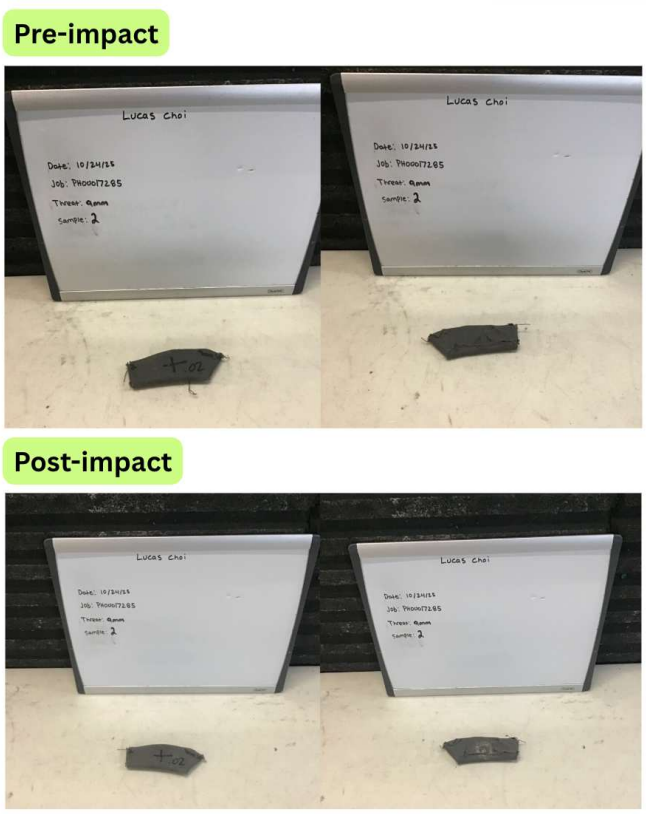


FIG. 15. Pre- and post impact condition of Sample 2 (Gray composite plate) following modified NIJ Level IIA ballistic testing.

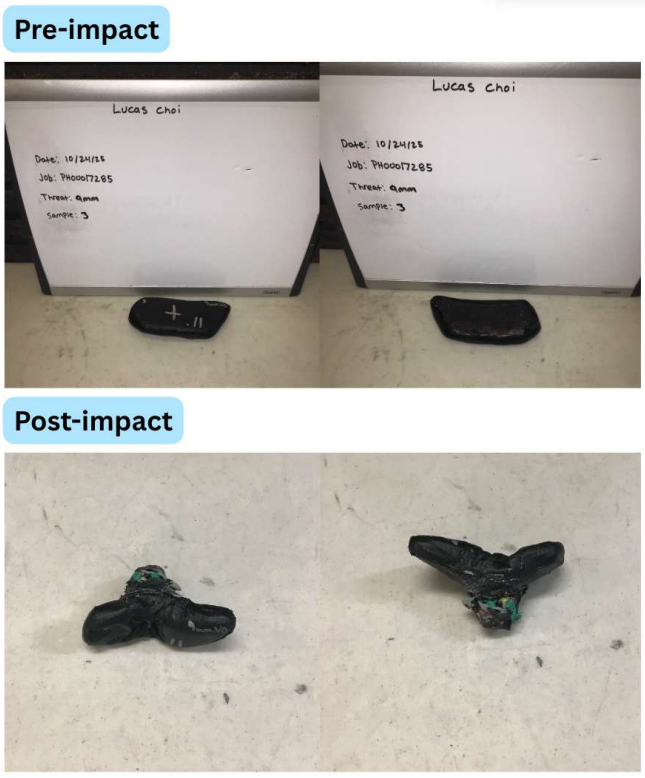


FIG. 16. Pre- and post impact condition of Sample 3 (Black composite plate) following modified NIJ Level IIA ballistic testing.

(1,195–1,255 ft/s), with no perforations observed. Samples 1, 2, 4, and 5 showed only superficial bullet spall and negligible BFD (< 1 mm), indicating effective energy dissipation by the front layers. However, the measured BFD of Sample 3 (57 mm) exceeded the 44 mm NIJ 0101.06 backface signature criterion and would therefore not satisfy the trauma requirement associated with NIJ Level IIA certification. This specimen is discussed separately as a thickness-controlled comparison and highlights the importance of considering both penetration resistance and backface deformation when evaluating ballistic performance.

These results establish coupon-level ballistic penetration resistance under the evaluated test conditions in an accredited third-party laboratory environment. Importantly, no projectile penetrations or preferential damage localizations were observed along inter-plate gap regions, indicating that the underlying Kevlar fiber continuity maintained ballistic integrity despite segmented plate geometry.

The W-Plate configuration demonstrated negligible BFD (< 1 mm), which is substantially below the 44 mm maximum backface signature specified under NIJ Standard 0101.06 for Level IIA soft armor [3]. This reduced deformation indicates limited measured backface deformation under the tested conditions. While direct comparison to certified soft-armor panels should be interpreted cautiously due to differences in specimen size and test configuration, the observed backface deformation results warrant further investigation through larger-scale and standardized ballistic testing.

Relative to representative NIJ Level IIA soft armor systems, which typically requires approximately 5 kg·m^{-2} areal density for 9 mm FMJ protection [8], a scaled lightweight sample (2.33 kg·m^{-2}, 9 g) resisted projectile penetration at an estimated 53.4% lower areal density; however, direct comparisons should be interpreted cautiously since testing was performed on reduced-scale coupons under modified NIJ-inspired conditions.

$$\text{Reduction (\%)} = \frac{5.0 - 2.33}{5.0} \times 100 = 53.4\% \qquad (1)$$

The absence of penetration across all coupons warrants further investigation of lightweight composite armor structures. Future studies should evaluate larger specimens, repeated-impact performance, and standardized ballistic testing protocols. With further optimization of layer count and resin ratio, the design could be adapted to modern ballistic vests, modular armor panels, or concealable protective apparel, potentially enabling improved multi–hit durability and reduced backface deformation in future configurations.

A. Qualitative Damage Localization Analysis

Post-impact evaluations included high-resolution photographs of the setup and impact, real-time or post-test video

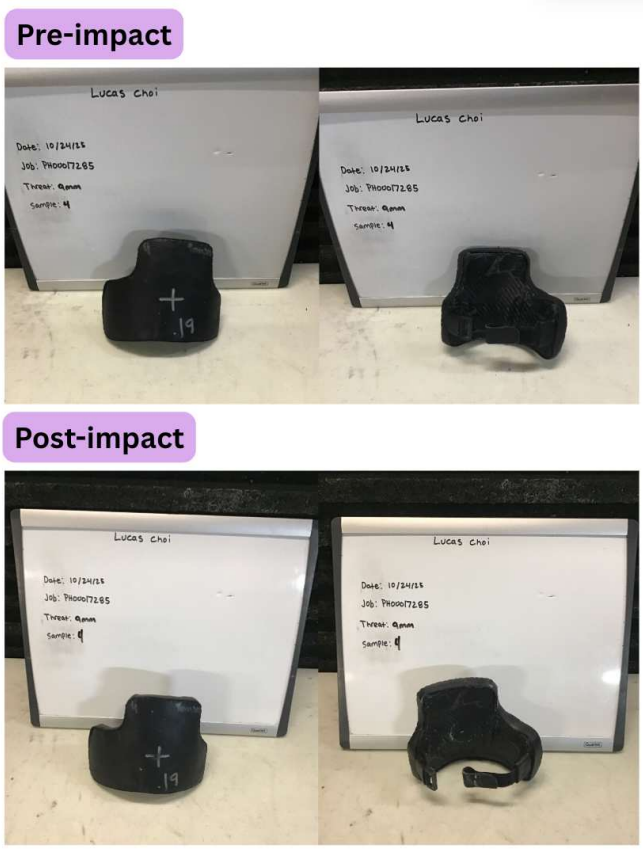


FIG. 17. Pre- and post impact condition of Sample 4 (Soft biceps composite guard) following modified NIJ Level IIA ballistic testing.



FIG. 18. Pre- and post impact condition of Sample 5 (Soft chestplate composite) following modified NIJ Level IIA ballistic testing.

footage, penetration analysis, measurement of BFD and documentation of shot grouping and damage spread. These results were used to assess the prototype's ballistic resistance, energy absorption characteristics, and failure modes. The collected data contributes to the overall understanding of performance under simulated real-world threat conditions, informing iterative design improvements for future prototypes.

B. Limitations

The ballistic evaluations were conducted on reduced-scale coupon specimens under modified NIJ Level IIA conditions rather than full certified wearable armor geometries. Therefore, the present study should not be interpreted as NIJ certification testing or direct equivalence to commercially certified armor systems. Sample dimensions and multi-hit spacing were limited by prototype size constraints. Consequently, the present results should be interpreted as an exploratory proof-of-concept evaluation rather than a statistically powered assessment of ballistic performance.

IV. CONCLUSION AND FUTURE WORK

This study demonstrates coupon-level ballistic resistance of a lightweight W-Plated Kevlar composite under modified NIJ Level IIA conditions at a mass of 131.5 g. Subsequent coupon-level testing indicates that ballistic feasibility can be achieved at substantially lower mass of 9.07 g (Sample 2).

Building on this result, future fabrication will prioritize W-Plating template-guided manual production scaled from the coupon geometry, with the aim of translating ultra-low-mass ballistic feasibility into larger-area, wearable configurations.

The W-Plating concept merits additional scrutiny, where future work will focus on larger-scale ballistic evaluation and ergonomic refinement to support materials optimization and protective applications, such as lightweight textile-based garments.

Ongoing research will explore graphene-based composites, boron- and carbon-nanotube reinforcements, and metamaterials to further reduce mass while maintaining high-strength protective layers. While graphene is exceptionally strong at the atomic scale, it presents challenges related to brittleness and fracture. Therefore, future investigations will examine methods for infusing graphene into lightweight fiber-based

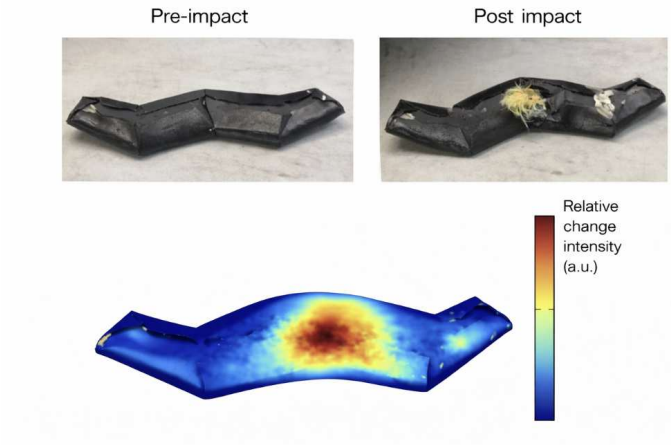


FIG. 19. Qualitative damage localization map derived from pre- and post-impact photographic analysis of the W-Plated composite. Warmer colors indicate regions of greater morphological change. The response appears distributed across a broader area of the specimen following impact.

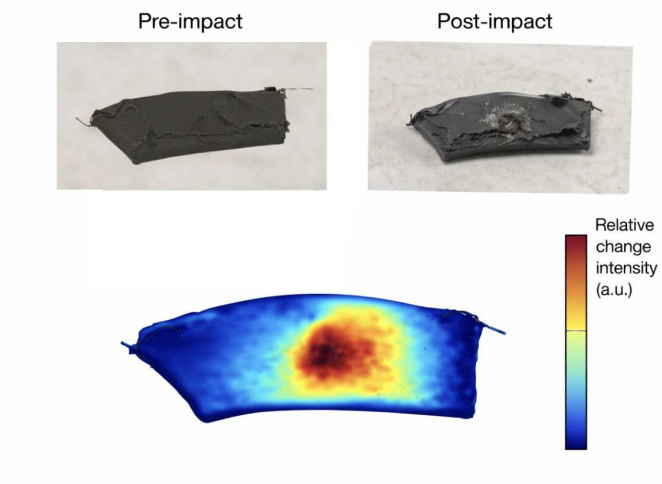


FIG. 20. Qualitative damage localization map derived from pre- and post-impact photographic analysis of the flat laminate specimen. Warmer colors indicate regions of greater morphological change. The response appears concentrated near the impact location.

matrices such as Kevlar or nylon to improve energy dissipation under ballistic and blunt-force loading. Graphene-enhanced shear-thickening fluids and hybrid composite systems will also be evaluated for their potential to further reduce BFD.

ACKNOWLEDGMENTS

We acknowledge Professor Addis A. Kidane (Columbia University, Civil Engineering and Engineering Mechanics) for conducting quasi-static compression testing at the Carleton Laboratory. We also thank Professor Udo D. Schwarz (Yale University, Mechanical Engineering and Materials Science) and Professor A. T. Charlie Johnson (University of Pennsylvania, Physics and Astronomy) for their mentorship and guidance throughout the development of this work. Additionally, we acknowledge Stanford University's Nano Shared Facilities (SNSF) and Dr. Tobi Beetz for access to microstructural characterization facilities and assistance with materials analysis.

We also extend our sincere gratitude to partial material and fabrication support provided through independent crowdfunding contributions from 11 backers, totaling $1,700. We thank Jameson Garcia, D'Angelo Watson, Alec Smith, Theo, Simon Lavigne, Joey, and Jacco for their generous support.

FUNDING

This research received no formal external funding. Partial material and fabrication support was provided through crowdfunding contributions.

DATA AVAILABILITY

All data generated or analyzed during this study are included in this published article and its supplementary information files. Complete raw ballistic velocity and BFD measurements are provided in the Supplementary Information.

ETHICS, CONSENT TO PARTICIPATE, AND CONSENT TO PUBLISH

No formal human-subject experimentation or participant recruitment was conducted in this study. Under applicable institutional and national guidelines, the activities described did not constitute formal human-subject research requiring Institutional Review Board (IRB) or ethics committee review because no participant recruitment, clinical procedures, or identifiable participant data were involved. All methods were carried out in accordance with relevant guidelines and regulations.

Ethics, Consent to Participate, and Consent to Publish declarations: Not applicable.

Clinical trial registration: Not applicable.

REFERENCES

[1] W. D. Callister and D. G. Rethwisch, *Materials Science and Engineering: An Introduction*, 10th ed. (Wiley, Hoboken, NJ, 2018).

[2] T. Sabir, "Kevlar – an overview," ScienceDirect Topics (2018), https://www.sciencedirect.com/topics/materials-science/kevlar.

[3]National Institute of Justice, "Ballistic resistance of body armor: Nij standard–0101.06," Tech. Rep. (U.S. Department of Justice, 2008) accessed January 2026.
[4]A. Kubik, Historia i Świat **9**, 83 (2020).
[5]M. Tsurtsumia, Byzantina Symmeikta **21**, 65 (2011).
[6]J. Gill, "Clad in steel: The evolution of plate armor in medieval europe and its relation to contemporary weapons development," Independent Research (2016).
[7]Y. Pan, M. Sang, J. Zhang, Y. Sun, S. Liu, Y. Hu, and X. Gong, Chemical Engineering Journal **452**, 139565 (2023).
[8]M. Karhankova, M. Adamek, L. Krstulović-Opara, V. Mach, P. Bagavac, P. Stoklasek, and A. Mizera, J. Compos. Sci. **8**, 415 (2024).
[9]R. O. J. Kollock, D. Hale, R. E. Vogelpohl, L. Kremer, C. Cox, J. Horner, and M. Allen, International Journal of Exercise Science **11**, 648 (2018).
[10]M. Greene, "Body armor: Protecting our nation's officers from ballistic threats," Natl. Inst. Justice (2018), national Institute of Justice.
[11]L. Tilsley, D. J. Carr, C. Lankester, and C. Malbon, J. R. Army Med. Corps **164**, 15 (2018).
[12]MIT School of Engineering, "Is it possible to make a batman suit?" (2024), accessed January 2026.
[13]C. Song, W. Fan, T. Liu, S. Wang, W. L. Song, and X. Gao, Compos. Part A Appl. Sci. Manuf. **153**, 106730 (2022).
[14]N. Abdelal and S. L. Donaldson, J. Compos. Mater. **12**, 311 (2018).
[15]D. Jaquet, A. B. Mazure, S. Armand, C. Charbonnier, J.-L. Ziltener, and B. Kayser, Technol. Cult. **49**, 169 (2016).
[16]M. Connors, T. Yang, A. Hosny, Z. Deng, F. Yazdandoost, H. Massaadi, D. Eernisse, R. Mirzaeifar, M. N. Dean, J. C. Weaver, C. Ortiz, and L. Li, Nature Communications **10** (2019), 10.1038/s41467-019-13215-0.
[17]P. Miranda, A. Pajares, and M. A. Meyers, J. Mater. Res. Technol. **8**, 1274 (2019).
[18]M. M. Yuan and B. H. Sun, Composite Structures **292**, 119237 (2025).
[19]Anonymous, "Illustrative image of historical segmented plate armor," (2026), accessed January 2026.
[20]E. A. S. K. Fernando, S. N. Niles, A. N. Morrison, P. Pranavan, I. U. Godakanda, and M. M. Mubarak, Int. J. Adv. Sci. Technol. Res. **1**, 434 (2015).
[21]C.-P. Chang, C.-H. Shih, J.-L. You, M.-J. Youh, Y.-M. Liu, and M.-D. Ger, Polymers **13**, 3080 (2021).
[22]M. Dada, B. E. Ghrewati, and M. R. Das, in *Recent Advances in Mechanical Engineering: Select Proceedings of ICRAMERD 2021* (Springer Nature Singapore, 2022) pp. 475–483.
[23]E. Camcı, M. Çalışkan, İ. Tural, Ö. Ergü, and F. Fındık, Int. J. Precis. Eng. Manuf. **25** (2023), 10.1007/s12541-023-00928-y.
[24]J. Trajkovski, R. Kunc, and I. Prebil, International Journal of Protective Structures **8**, 524 (2017).
[25]G. Langdon, A. Curry, V. Shekhar, A. Siddiqui, C. Murray, and C. von Klemperer, Ce/Papers **4**, 1499 (2021).
[26]R. Oliwa, Materials **13**, 3726 (2020).